

## MECHANICAL AND CHEMICAL STUDIES OF $\text{Al}_2\text{O}_3$ -Ti COMPOSITES FOR THEIR USE AS A BONE SUBSTITUTE

Elizabeth Refugio-García<sup>1</sup>, Gerardo Vázquez-Huerta<sup>1</sup>,  
José Miranda-Hernández<sup>2</sup>, Jessica Osorio-Ramos<sup>1</sup>, José Rodríguez-García<sup>3</sup>,  
Enrique Rocha-Rangel<sup>3</sup>, ✉

<https://doi.org/10.23939/chcht15.04.591>

**Abstract.** Alumina-based composites reinforced with titanium were manufactured by powder techniques. Characterizations indicate that titanium content affects densification which in turn causes positive effects on hardness and toughness. Microstructure presents grains of irregular shape and small sizes. Electrochemical impedance spectroscopy indicates that additions of titanium on  $\text{Al}_2\text{O}_3$  enhance its corrosion resistance.

**Keywords:**  $\text{Al}_2\text{O}_3$ , bioceramics, mechanical properties, chemical properties.

### 1. Introduction

For several years, numerous researchers have focused their study to strengthen a ceramic matrix through addition of different materials whether metallic, ceramic or intermetallic. This reinforcement is reflected in the improvement of the fracture toughness and in some cases of other properties such as corrosion resistance. Thus, alumina matrix compounds reinforced with the addition of different reinforcement materials have been studied: [1-6], nickel [7], molybdenum [8], silver [9], and titanium [10-11]. In research reports it has been informed that with the addition of elements on the ceramic matrix and using powder techniques, significant improvement in fracture toughness are achieved; as is the case when making use of uniaxial compaction and conventional sintering at 1723 K,

the toughness value increases from 4.84 to 6.9 and 12  $\text{MPa}\cdot\text{m}^{0.5}$ , with additions of 15, 20 and 25 wt % of molybdenum, respectively, in the alumina matrix. However, not only the content of the reinforcement allows an improvement in properties – some researchers have found that by employing specialized treatments such as hot compaction or spark plasma sintering the mechanical properties can also be improved [12-15]. For example, in the case of alumina-niobium composites, with contents of 10 wt % niobium and sintering by hot pressing, fracture toughness has reached values of 8  $\text{MPa}\cdot\text{m}^{0.5}$  [16].

Because human bone is a ceramic material with a relatively low fracture toughness of 1.8  $\text{MPa}\cdot\text{m}^{0.5}$ , several researchers have proposed to make composites with good fracture toughness for their possible application as biomaterials. Yoshida [17] studied the mechanical properties of zirconia-AISI316L steel compound with metal contents of up to 30 vol %. With this high metal concentration, he managed to increase the fracture toughness from 5 to 6  $\text{MPa}\cdot\text{m}^{0.5}$ . Subsequently, Mishina [18] has evaluated the mechanical properties of the same system with gradient function, reaching fracture toughness values up to 14  $\text{MPa}\cdot\text{m}^{0.5}$ . However, in both cases biocompatibility problems were found due to the toxicity of steel in the human body. Also, Oshkour [19] has studied mechanical properties of composites of calcium silicate with the additions of Ti-55Ni and Ti-6Al-4V alloys for hard tissues replacement, achieving good results. Apart from that, Cook [20] informed about density values of 1.06 and fracture toughness of 1.6  $\text{MPa}\cdot\text{m}^{0.5}$  in trabecular bones. On the other hand, Norman [21] has reported that the compact human bones have densities of 1.8  $\text{g}\cdot\text{cm}^{-3}$  and fracture toughness of 4.05–4.32  $\text{MPa}\cdot\text{m}^{0.5}$ .

Titanium is a commonly used biomaterial for the manufacture of prostheses due to its properties such as high tensile strength, good fatigue strength, ductility and toughness compared with ceramic and polymeric materials. Its density is low, corresponding to 4.7  $\text{g}\cdot\text{cm}^{-3}$  compared to the high densities of some alloys used as biomaterials, such as 7.9  $\text{g}\cdot\text{cm}^{-3}$  of stainless steel,

<sup>1</sup> Materials Department, Universidad Autónoma Metropolitana, Avenida San Pablo 180, Col. Reynosa-Tamaulipas, CDMX, 02200, México

<sup>2</sup> Industrial Materials Research and Development Laboratory, Universidad Autónoma del Estado de México, Centro Universitario UAEM Valle de México,

Atizapán de Zaragoza, Estado de México, 54500, México

<sup>3</sup> Manufacture Department, Universidad Politécnica de Victoria, Av. Nuevas Tecnologías 5902, Parque Científico y Tecnológico de Tamaulipas, Ciudad Victoria, Tamaulipas, 87138, México

✉ [erochar@upv.edu.mx](mailto:erochar@upv.edu.mx)

© Refugio-García E., Vázquez-Huerta G., Miranda-Hernández J., Osorio-Ramos J., Rodríguez-García J., Rocha-Rangel E., 2021

8.3 g·cm<sup>-3</sup> of the Co-Cr-Mo alloy, or 9.2 g·cm<sup>-3</sup> of the Co-Ni-Cr-Mo alloy. Thus, the novelty of this research is centered on the production of alumina-based ceramics with the addition of titanium through a simple and economical method of processing so that the resulting material meets the physical and chemical characteristics to be used as biomaterial.

## 2. Experimental

Al<sub>2</sub>O<sub>3</sub>/Ti composites were made using titanium powders (Aldrich, 99.99% purity, 5–10 μm particle size) and alumina (Aldrich, 99.99% purity, 1 μm particle size). With the idea of determining the effect of Ti on the physical and chemical properties of the fabricated composite, titanium was added in the proportions of 0.0, 0.5, 1, 2 and 3 wt % in the alumina matrix. Each different composition mixture was subjected to a high energy milling process, in a planetary type mill (Retsch, PM100 German), using isopropyl alcohol as a control agent; ZrO<sub>2</sub> spheres of 10 and 13 mm in diameter were used as grinding media; the grinding time was 3 h and carried out at 300 rpm. The powders resulting from the milling were molded by uniaxial compaction at 350 MPa (Montequipo, LAB-30-T, Mexico), into cylindrical pellets of 2 cm in diameter by 0.3 cm thick. Conformed samples were subjected to sintering treatments for 1 h at the temperatures of 1673, 1773 and 1873 K, as well as for 2 and 3 h at 1673 K, all of them in a protective atmosphere of nitrogen in an electric furnace (Carbolite, RHF17/3E, England). Before the characterization of the sintered samples, all of them were prepared by SiC papers grinding and polishing using 3 μm and 1 μm diamond suspension. Then physical characterization of the cermets was carried out to determine the density and interconnected porosity, according to the Archimedes' principle [22]. Samples were characterized by X-ray diffraction (XRD) measurements performed on a Phillips-X'Pert diffractometer using CuKα radiation. The fracture toughness was determined using the indentation fracture method in microhardener equipment (Wilson Instruments, S400, Japan), in agreement with international standards [23]. The hardness and elastic modulus also were determined according to standards [24, 25]. The microstructural characteristics of the cements were observed by SEM (JEOL, JSM 6300, Japan). Corrosion susceptibility studies were carried out on the studied materials by means of electrochemical impedance spectroscopy (EIS) assisted by potentiodynamic polarization techniques carried out in a potentiostat-galvanostat, VersaSTAT-4, USA, equipment. Finally, microstructure and values of density, porosity, hardness, fracture toughness and elastic modulus, as well as

corrosion resistance of the fabricated composites were compared with the microstructure and values of these same properties of compact bone.

## 3. Results and Discussion

### 3.1. Density

Fig. 1 shows density values of sintered composites as a function of Ti content in the sample. In this figure, it is observed that the highest density value is obtained for the contents of 0.5 wt % titanium in the composite, regardless of sintering time or temperature. For higher titanium contents in the sample the density tends to decrease. On the other hand, we observed a significant effect of the temperature increase on the densification of the samples, the sample that best densifies is the one that was treated at the highest temperature (1873 K), followed by the sample sintered at 1773 K. In the case of sintered samples at 1673 K at different times, the best densities were obtained in samples sintered for a longer time. In the case of the effect of temperature and time on densification, a logical behavior was observed since diffusion phenomena are favored by temperature and time increases. Because titanium is a metal, this favors the conduction of heat to the interior of the sample, which brings with it a better densification of the sample. However, at contents greater than 0.5 wt %, it is likely that because titanium greatly favors diffusion, this implies abnormal grain growth of the sample, thereby causing deterioration in the densification thereof. In all cases the density of the compounds is well above the density of the cortical bone, which is 1.8 g·cm<sup>-3</sup> (represented by the dashed line at the bottom of Fig. 1) [26].

### 3.2. Porosity

Fig. 2 shows the porosity values of sintered composites as a function of Ti content in the sample. The graph shows that sintering conditions at high temperatures (1773 and 1873 K) generate bodies with porosity values close to or less than 10 % for samples where titanium was added. In the sintered samples at 1673 K, the porosity of the alumina decreases considerably when titanium is added at different sintering times. However, the decrease in density does not appear to be affected by the amount of titanium in the composite, since for contents greater than 0.5 wt % of titanium this decrease is not significant. Porosity is important when designing bodies for bone regeneration, because values higher than 10 % of porosity in ceramics are good indicators of interconnectivity [27], so the greater the porosity, the higher probability of interconnection between pores. The porosity values of the cortical bones are approximately 15 % (represented by the dashed line in the middle of the Fig. 2) [26].

### 3.3. X-Ray Diffraction

Sintered samples were characterized by X-ray diffraction (XRD) measurements performed on a Phillips-X'Pert diffractometer using CuK $\alpha$  radiation ( $k = 0.15406$  nm) source with a working voltage of 40 kV. The measurement was performed between 10 and 100° with a scan rate of 0.02  $\theta$  and integration time of 3 s per step. Fig. 3 presents the XRD patterns of the Al<sub>2</sub>O<sub>3</sub>-based

studied samples with 0 and 3 wt % Ti sintered at 1673 K for 2 h. In the pattern corresponding to the sample with 0 %Ti, the presence of a single compound, which corresponds to alumina, is observed. The diffraction pattern found in the upper part of Fig. 3 corresponds to the sample with 3 wt% Ti; in addition to the alumina, the presence of the aggregate Ti is observed, thus verifying the presence of the second phase particles added to the composites.

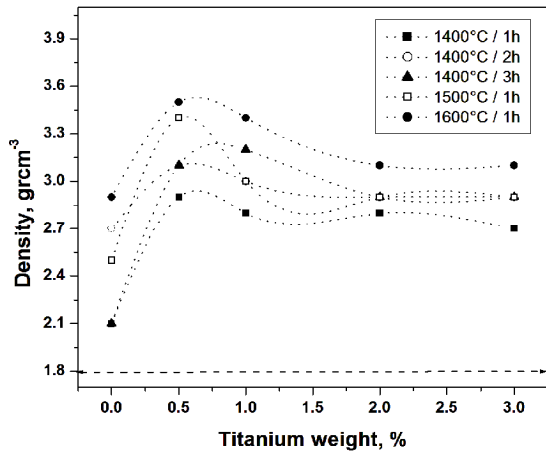


Fig. 1. Density of sintered samples as a function of Ti content

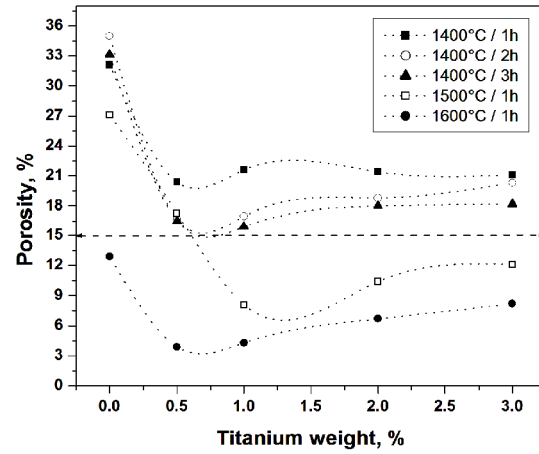


Fig. 2. Porosity of sintered samples as a function of Ti content

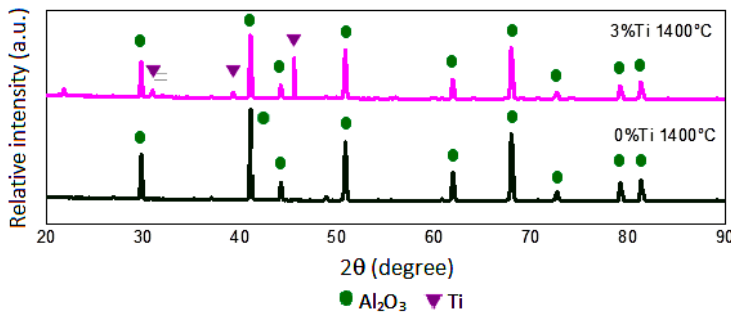


Fig. 3. X-ray diffraction patterns of sintered materials at 1673 K for 2 h

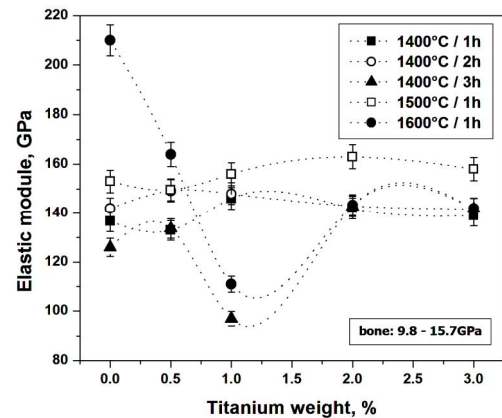


Fig. 4. Elastic modulus (flexion) of sintered samples as a function of Ti content

### 3.4. Elastic Modulus

The elastic modulus (determined in flexural conditions) was measured in 2 cm long rectangular samples with a universal testing machine (Gunt-WP300) using three points technique, with span of 1.8 cm. Fifteen tests were made for three samples. Fig. 4 presents the results of this test carried out on sintered composites under

different conditions of this work. In this figure, it may be observed that the amount of titanium in the sample slightly influences the final value of elastic modulus of the composites. For the sintered sample at 1873 K during 1 h, there is a strong drop in the elastic modulus for the composites with 0, 0.5 and 1 wt % of titanium, increasing the elastic modulus for the samples with 2 and 3 wt % of titanium. For the rest of the sintering conditions and

chemical compositions, there are no significant variations of the elastic modulus; very uniform values appear in all cases. The elastic modulus for cortical bone determined in flexion varies from 9.8 to 15.7 GPa [26]. For the materials manufactured here the elastic modulus is well above these values. This implies that the material manufactured here will be able to withstand a high degree of load per unit area with a low deformation index, which gives it a great rigidity, superior to that of the cortical bone. On the other hand, in this figure a strong fall in the elastic module for the sample with 1 wt % of titanium, sintered at 1673 K for 3 h and 1873 K for 1 h is observed, which are the most extreme conditions in terms of sintering time and temperature. These working conditions surely caused excessive grain growth, making the sample less rigid. This situation is confirmed by the density results, because also for this samples in the sintering conditions mentioned above less densification was achieved.

### 3.5. Microhardness

The hardness was measured in cylindrical pellets of 2 cm in diameter by 0.3 cm thick with a Vickers Hardness Tester (Wilson Instruments, S400) using a load of 9.8 N with 15 s holding time. Twenty indentations were made for three samples. Fig. 5 presents values of microhardness measurements in the materials obtained in this study. In this figure it was found that in all cases the microhardness of the materials manufactured here is well above the value of 350 HV, which is the microhardness value of cortical bone (represented by the dashed line at the bottom of the figure) [26]. In the figure it may be observed that for the contents of 0.5 wt % Ti in the sample, the hardness rises considerably, decreasing for higher Ti contents. With regard to the influence of the sintering conditions, the increase in temperature has an important influence on higher values of microhardness. However, the sintering time does not seem to have a significant effect on this property, because there are no greater variations of the microhardness with respect to the sintering time. Once again, the effect of temperature on the phenomena of diffusion is evident here due the fact that the highest microhardness value was reached in the samples that were treated at higher temperatures. Another important observation presented with the general results of the hardness of the samples is that there is a good correlation with the density values. This means that better-densified bodies have better mechanical behavior. On the other hand, when the density decreases (increased porosity), the hardness of the composites also decreases. This good correspondence of the hardness with the density and the porosity makes us suppose that the obtained results are reliable, because it is to be expected as already

commented before, that dense bodies provide materials with better mechanical behavior.

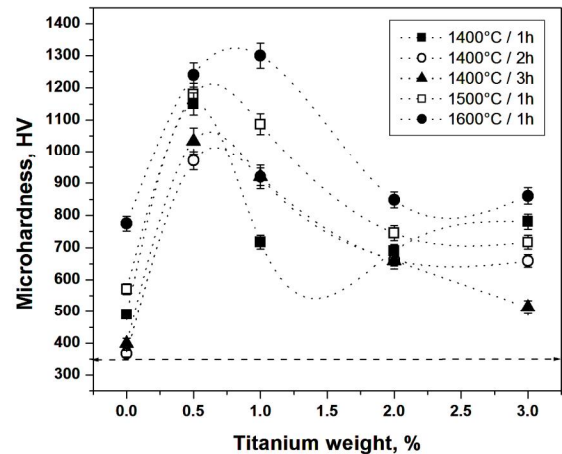


Fig. 5. Microhardness of sintered samples as a function of Ti content

### 3.6. Fracture Toughness

The fracture toughness was estimated with a Vickers Hardness Tester (Wilson Instruments, S400) using the indentation technique under the load of 9.8 N with 15 s holding time. Twenty indentations were made for three samples. The measurements of the diagonals and cracks have been done on the JEOL, JSM 6300 scanning electron microscope. The fracture toughness has been calculated using the Miyoshi's equation [28].

$$K_{IC} = 0.018 \left( \frac{E}{H} \right)^{0.5} \left( \frac{P}{c^{1.5}} \right) \quad (1)$$

where  $K_{IC}$  is the fracture toughness,  $\text{MPa}\cdot\text{m}^{0.5}$ ;  $H$  is the Vickers hardness, GPa;  $E$  is the modulus of elasticity, GPa;  $P$  is the applied load, N;  $c$  is the average length of the cracks obtained from the Vickers fingerprint tips, m.

The results of fracture toughness measurements in fabricated composites are presented in Fig. 6. Fracture toughness of compact cortical bone, the value of which is  $4.3 \text{ MPa}\cdot\text{m}^{0.5}$  (represented by the dashed line at the middle of the Fig. 6) [26] is presented in the same figure. The figure shows good influence of titanium additions on fracture toughness of alumina, as well as the effect of the sintering conditions. It is important to clarify that in order to provide a material that is a bone substitute, it must provide at least the same properties of the bone, and fracture toughness is of the utmost importance. Thus, conditions which provide better fracture toughness than those of bone are sintering conditions of 1773 and 1873 K during 1 h, as well as sintering at 1673 K for 3 h. In regard to the amount of titanium in the composite, increases of

this metal considerably favor the fracture toughness of the composites due to the higher ductility of titanium than that of alumina.

Fig. 7a shows a photomicrograph of a typical indentation mark, while Fig. 7b shows an enlargement in one of the corners of the indentation mark showing a crack.

### 3.7. Microstructure

Fig. 8 shows the microstructure of composites with different titanium contents sintered at 1773 K during 1 h. Microstructures with irregularly shaped grains are observed in all samples, with average sizes ranging from 1 micron to slightly less than 10 microns. For the control sample (0 wt% Ti) a partially sintered microstructure was observed, which means that the sintering conditions were not high enough to reach a good densification of this ceramic. For the microstructures with titanium additives

different situation occurs for all experiments. Better consolidated bodies in the samples were observed and the situation improved with the increase of the sintering times (Fig. 9). This situation can be explained by the fact that titanium, which is a good heat conductor, provides diffusion between the particles of the material, although it was possible to perceive a minimum increase of the grain size as a function of the sintering time. In general, it can be said that the microstructure is very homogeneous, improving this homogeneity at higher sintering times. Likewise, no significant presence of porosity is observed. Fig. 9d shows the microstructure of cortical compact bone, in which a very fine grain size and low porosity is observed. Certainly, the microstructure of the bone is very different from that of the composites manufactured here. However, it has already been observed that these composites combine and even improve the physical and mechanical characteristics of the cortical bone.

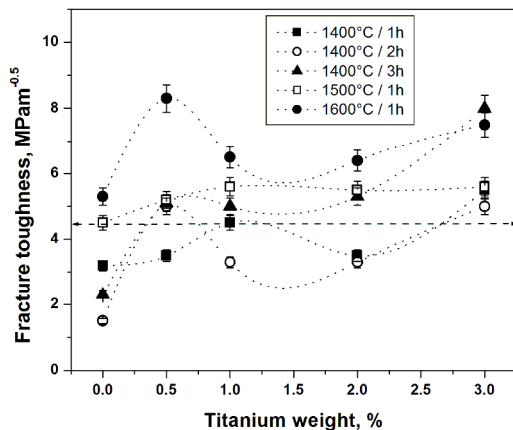


Fig. 6. Fracture toughness of sintered samples as a function of Ti content

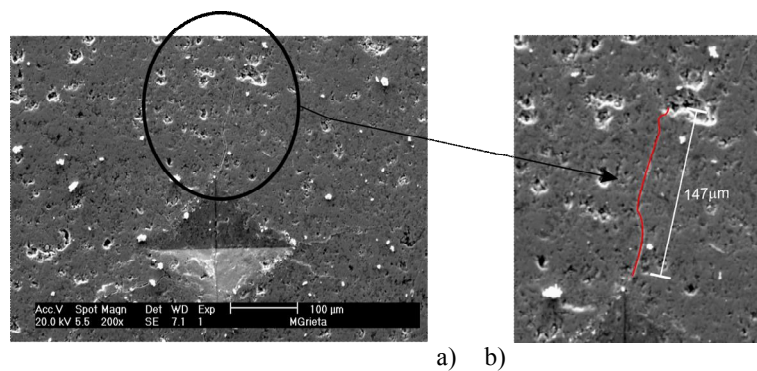


Fig. 7. Indentation mark (a) and corners of the indentation mark (b) showing a crack

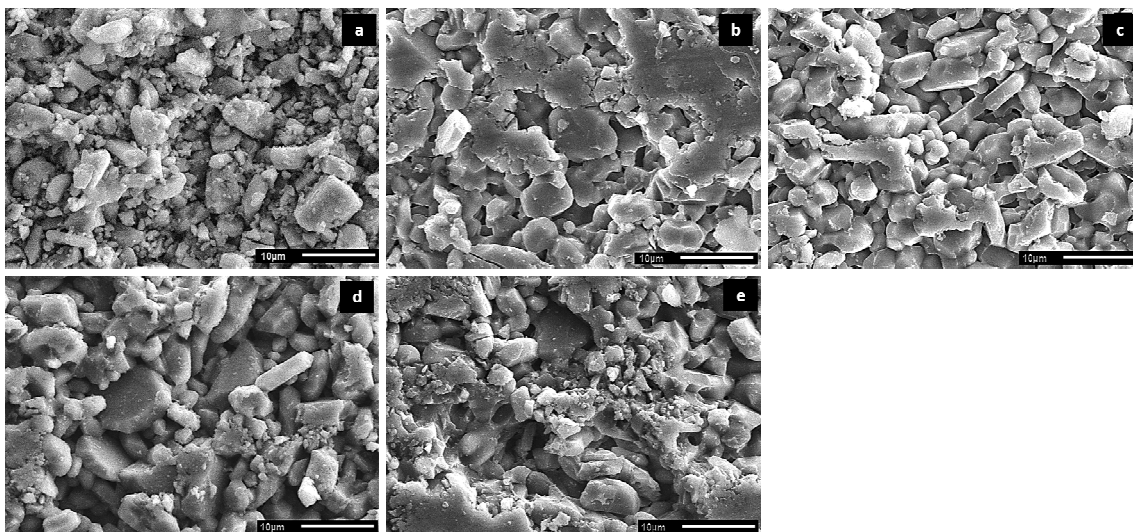
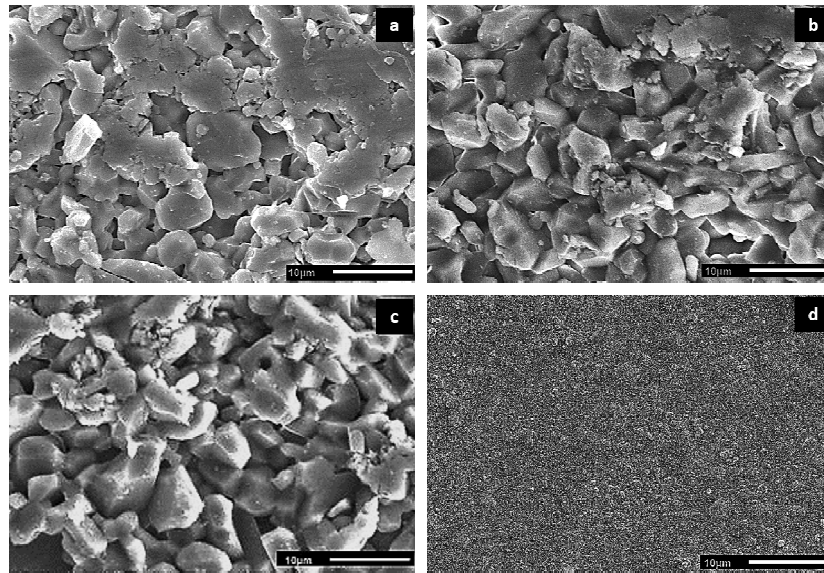
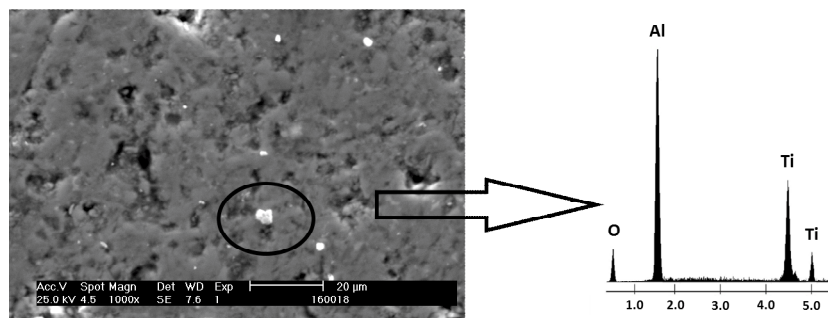


Fig. 8. Microstructure of cermets with different titanium contents, sintered at 1773 K during 1 h: Al<sub>2</sub>O<sub>3</sub> (a); Al<sub>2</sub>O<sub>3</sub>-0.5 wt% Ti (b); Al<sub>2</sub>O<sub>3</sub>-1.0 wt% Ti (c), Al<sub>2</sub>O<sub>3</sub>-2.0 wt% Ti (d) and Al<sub>2</sub>O<sub>3</sub>-3.0 wt% Ti (e)



**Fig. 9.** Microstructure of cermet with 0.5 wt % of titanium, sintered at 1773 K at different times: 1h (a); 2h (b); 3 h (c) and cortical compact bone (d)



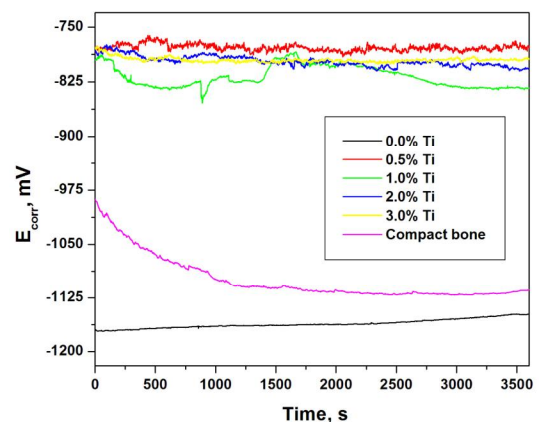
**Fig. 10.** EDS spectrum of the  $\text{Al}_2\text{O}_3$ -2.0 wt% Ti sample sintered at 1773 K for 2 h

Fig. 10 shows a microstructure with a black circle exhibiting a white particle inside, for this area an analysis by energy dispersive spectroscopy (EDS) was considered to be carried out, aimed to find out the chemical elements present there. In the EDS resulting spectrum, the presence of Ti, Al and O, chemical elements that match up to the  $\text{Al}_2\text{O}_3/\text{Ti}$  composite is perceived, verifying in this way the presence of titanium in the composite.

In order to evaluate the behavior of the resistance to degradation as a function of the titanium content in the composites and given the above conclusions, degradation studies were performed on  $\text{Al}_2\text{O}_3$ -Ti compounds that were sintered at 1773 K during 1 h, for each studied compositions.

### 3.8. Corrosion Potential: Degradation Potential

Fig. 11 shows the  $E_{corr}$  vs. time curves for each studied composition. The figure shows that composites  $\text{Al}_2\text{O}_3$ -Ti with highest titanium content are the least likely



**Fig. 11.** Corrosion potential of sintered composites at 1773 K for 1 h, as a function of titanium content

to corrode or degrade, because their corrosion potential is between -850 and -750 mV, having a potential drop to -1150 mV for materials without titanium addition. In the same graph the spectrum corresponding to the corrosion potential of the compact bone is presented; this

potential has the value of -975 mV, which is above the potential of -1150 mV corresponding to the corrosion potential of the  $Al_2O_3$ -base composites, which indicates that  $Al_2O_3$ -0 wt% Ti composite is more susceptible to degradation than bone. However, when Ti is added to  $Al_2O_3$ , spectra have a potential greater than the potential exhibited by the bone, which implies that the titanium in the ceramic matrix reinforces this resistance to degradation.

### 3.9. Electrochemical Impedance Spectroscopy

Fig. 12 shows the electrochemical impedance results in form of Nyquist diagrams ( $Z_{imag}$  vs.  $Z_{real}$ ) for  $Al_2O_3$ -Ti composites, considering that composites were immersed in a 0.9 % saline solution. The diagrams in Fig. 12a reveal that the load transfer resistance value ( $Z_{real}$ ) increases considerably by several orders of magnitude for composites containing 0.5 wt % of titanium. This rise in  $Z_{real}$  value indicates that composites with a 0.5 wt% Ti are those materials that show less degradation in a saline medium similar to the human body. Fig. 12a also shows the impedance results in the form of Nyquist diagram for the compact bone which was immersed in a physiological solution; in this diagram it is possible to observe a

semicircle where the value of load transfer resistance  $Z_{real}$  is of the order of 12,000  $\Omega$ , which is much lower than the corresponding value of 80,000  $\Omega$  of the cermet with 0.5 wt% Ti, and indicates that the bone presents a lower resistance to degradation compared to  $Al_2O_3$ -0.5 wt% Ti composites.

Fig. 12b corresponds to an extension of the Nyquist diagrams of the  $Al_2O_3$ -Ti composites from Fig. 12a; this was done with the objective of better observing the size of the semicircles for each composition. It is perceived from Fig. 12b that the size of the semicircle is greater for composites that contain 1, 2 and 3 wt % of titanium than that of the bone, so it is possible to conclude that with addition of titanium in the ceramic matrix, there is less degradation of the composite in the physiological solution. However, the semicircle corresponding to  $Al_2O_3$ -0.5 wt% Ti sample is much larger than any other. Knowing that a denser material exhibits greater resistance to degradation in various environments, and observing Fig. 1, the highest density value is obtained for the samples with 0.5 wt % of titanium in the composite, regardless of sintering time or temperature, whereas for higher titanium contents in the sample the density tends to decrease, hence the better resistance to degradation of  $Al_2O_3$ -0.5 wt% Ti sample.

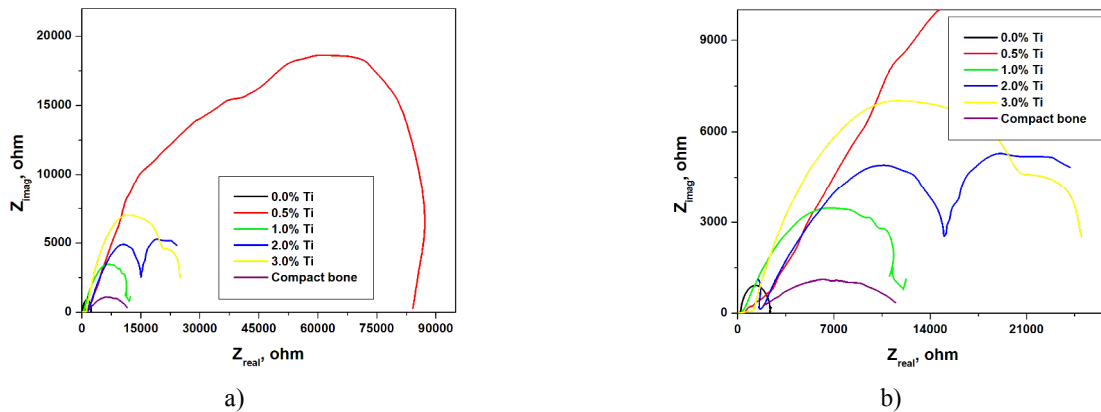


Fig. 12. Nyquist graphs (a) corresponding to the behavior of the  $Al_2O_3$ -Ti composites and enlargement of Nyquist diagrams (b) of the  $Al_2O_3$ -Ti composites

### 4. Conclusions

In this work,  $Al_2O_3$ -Ti composites were manufactured through powder techniques, in order to obtain a material with physical and chemical characteristics of cortical bone. From the results obtained, it is concluded that the sintering time and temperature affect directly and proportionally mechanical properties ( $HV$ ,  $K_{IC}$ ,  $E$ ) of fabricated composites. Likewise, it was determined that the titanium content has a direct positive effect on porosity as well as microhardness and fracture toughness. On the other hand, composites present a

decrease in the percentage of interconnected porosity when sintering time and temperature increases, whereas density is higher. From the results of electrochemical impedance spectroscopy, it follows that additions of titanium on  $Al_2O_3$  enhance the corrosion resistance of the composite in saline media similar to those of the human body, hence the application of the  $Al_2O_3$ /Ti composites as a bone substitute is viable. Finally, composites with 0.5 wt % sintered at 1773 K during 1 h are the ones that present similar properties to those of the bone (1.8  $g \cdot cm^{-3}$  density, 10–15 % porosity, 350 HV hardness, 4.3  $MPa \cdot m^{0.5}$  fracture toughness).

## References

- [1] Daguano J., Santos C., Souza R. *et al.*: *Int. J. Refract. Met. H.*, 2007, **25**, 374. <https://doi.org/10.1016/j.ijrmhm.2006.12.005>
- [2] Wu Y., Zhang Y., Huang X., Guo J.: *J. Eur. Ceram. Soc.*, 2001, **21**, 581. [https://doi.org/10.1016/S0955-2219\(00\)00245-4](https://doi.org/10.1016/S0955-2219(00)00245-4)
- [3] Wang L., Shi J., Hua Z. *et al.*: *Mater. Lett.*, 2001, **50**, 179. [https://doi.org/10.1016/S0167-577X\(01\)00221-X](https://doi.org/10.1016/S0167-577X(01)00221-X)
- [4] Miyazaki H., Yoshizawa Y., Hirao K.: *Mater. Lett.*, 2004, **58**, 1410. <https://doi.org/10.1016/j.matlet.2003.09.037>
- [5] Liu C., J., Sun J., Zhang X.: *Ceram. Int.*, 2007, **33**, 1319. <https://doi.org/10.1016/j.ceramint.2006.04.014>
- [6] Liu C., Zhang J., Sun J. *et al.*: *Ceram. Int.*, 2007, **33**, 1149. <https://doi.org/10.1016/j.ceramint.2006.03.018>
- [7] Sekino T., Nakajima T., Niihara K.: *Mater. Lett.*, 1996, **29**, 165. [https://doi.org/10.1016/S0167-577X\(96\)00136-X](https://doi.org/10.1016/S0167-577X(96)00136-X)
- [8] Konopka K., Maj M., Kurzydowski K.: *Mater. Charact.*, 2003, **51**, 335. <https://doi.org/10.1016/j.matchar.2004.02.002>
- [9] Chou W., Tuan W.: *J. Eur. Ceram. Soc.*, 1995, **15**, 291. [https://doi.org/10.1016/0955-2219\(95\)90351-I](https://doi.org/10.1016/0955-2219(95)90351-I)
- [10] Wu C., Wang Z., Li Q. *et al.*: *J. Alloys Compd.*, 2014, **617**, 729. <https://doi.org/10.1016/j.jallcom.2014.08.007>
- [11] Mas-Guindal M., Benko E., Rodriguez M.: *J. Alloys Compd.*, 2008, **454**, 352. <https://doi.org/10.1016/j.jallcom.2006.12.105>
- [12] Ji Y., Yeomans J.: *J. Eur. Ceram. Soc.*, 2002, **22**, 1927. [https://doi.org/10.1016/S0955-2219\(01\)00528-3](https://doi.org/10.1016/S0955-2219(01)00528-3)
- [13] Lalonde J., Scheppokat S., Janssen R., Claussen N.: *J. Eur. Ceram. Soc.*, 2002, **22**, 2165. [https://doi.org/10.1016/S0955-2219\(02\)00031-6](https://doi.org/10.1016/S0955-2219(02)00031-6)
- [14] Yao X., Huang Z., Chen L. *et al.*: *Mater. Lett.*, 2005, **59**, 2314. <https://doi.org/10.1016/j.matlet.2005.03.012>
- [15] Guichard J., Tillement O., Mocellin A.: *J. Eur. Ceram. Soc.*, 1998, **18**, 1143. [https://doi.org/10.1016/S0955-2219\(98\)00009-0](https://doi.org/10.1016/S0955-2219(98)00009-0)
- [16] De Portu G., Guicciardi S., Melandri C., Monteverde F.: *Wear*, 2007, **262**, 1346. <https://doi.org/10.1016/j.wear.2007.01.010>
- [17] Yoshida K., Mishina H., Sasaki S. *et al.*: *J. Jpn. I. Met.*, 2005, **69**, 793. <https://doi.org/10.2320/jinstmet.69.793>
- [18] Mishina H., Inumaru Y., Kaitoku K.: *Mater. Sci. Eng. A*, 2008, **475**, 141. <https://doi.org/10.1016/j.msea.2007.05.004>
- [19] Oshkour A., Pramanik S., Shirazi S. *et al.*: *Sci. World J.*, 2014, **2014**, 9. <https://doi.org/10.1155/2014/616804>
- [20] Cook R., Zioupos P.: *J. Biomech.*, 2009, **42**, 2054. <https://doi.org/10.1016/j.jbiomech.2009.06.001>
- [21] Norman T., Vashisth D., Burr D.: *J. Biomech.*, 1995, **28**, 309. [https://doi.org/10.1016/0021-9290\(94\)00069-G](https://doi.org/10.1016/0021-9290(94)00069-G)
- [22] ASTM B962-17: Standard Test Methods for Density of Compacted or Sintered Powder Metallurgy (PM) Products Using Archimedes' Principle, Pennsylvania, USA, 2017.
- [23] ASTM C1421-18: Standard Test Methods for Determination of Fracture Toughness of Advanced Ceramics at Ambient Temperature, Pennsylvania, USA, 2018.
- [24] ASTM C1327-15: Standard Test Method for Vickers Indentation Hardness of Advanced Ceramics, Pennsylvania, USA, 2015.
- [25] ASTM E1876-15: Standard Test Method for Dynamic Young's Modulus, Shear Modulus, and Poisson's Ratio by Impulse Excitation of Vibration, Pennsylvania, USA, 2015.
- [26] Kutz M.: *Standard Handbook of Biomedical Engineering and Design*, McGraw-Hill, New York 2013.
- [27] Polo-Corrales L., Latorre-Estevés M., Ramirez-Vick J.: *J. Nanosci. Nanotechnol.*, 2014, **14**, 15. <https://doi.org/10.1166/jnn.2014.9127>
- [28] Miyoshi T., Sagawa N., Sassa T.: *Trans. Jpn. Soc. Mech. Eng. A*, 1985, **51**, 2489. <https://doi.org/10.1299/kikaia.51.2489>

*Received: April 14, 2020 / Revised: May 17, 2020 / Accepted: August 01, 2020*

### МЕХАНІКО-ХІМІЧНІ ДОСЛІДЖЕННЯ КОМПОЗИТІВ $Al_2O_3$ -Ti ДЛЯ ЇХ ЗАСТОСУВАННЯ ЯК КІСТКОВОГО ЗАМІСТНИКА

**Анотація.** Порошковими методами синтезовані композити на основі глинозему, зміцнені титаном. Показано, що вміст титану впливає на ущільнення, що в свою чергу позитивно впливає на твердість та в'язкість. Мікроструктурним аналізом встановлено, що зерна мають неправильну форму та невеликі розміри. За допомогою спектроскопії електрохімічного імпедансу визначено, що добавки титану до  $Al_2O_3$  підвищують його корозійну стійкість.

**Ключові слова:**  $Al_2O_3$ , біокераміка, механічні властивості, хімічні властивості.